

## Hazard implications of the late arrival of the 1945 Makran tsunami

C. P. Rajendran<sup>1\*</sup>, M. V. Ramanamurthy<sup>2</sup>,  
N. T. Reddy<sup>2</sup> and Kusala Rajendran<sup>1</sup>

<sup>1</sup>Centre for Earth Sciences, Indian Institute of Science,  
Bangalore 560 012, India

<sup>2</sup>Integrated Coastal and Marine Area Management,  
Department of Ocean Development, Ministry of Earth Sciences,  
Chennai 601 302, India

**The 1945 Makran earthquake is known to have generated tsunami surges that affected the coasts of Iran, Pakistan, Oman and India. However, there is a significant delay in tsunami arrivals at various coastal sites with respect to the origin time of the earthquake. We explored the archival data to obtain arrival times and run-up heights at some important port cities along the Pakistan and Indian coasts. Numerical model for wave propagation based on the available rupture parameters predicts arrival times 17 and 28 min ahead of the actual arrival of the first surge at Karachi and Pasni respectively. There was also a significant discrepancy (>3 h) between the origin time of the earthquake and the observed arrival times of the second wave at various locations, which was the largest of the surges. We attribute this disparity in arrival time of the tsunami surges to submarine landslides triggered by the earthquake. Submarine slide-triggered tsunami is an underestimated threat in the Indian Ocean, and therefore, the regional tsunami hazard models of both the Arabian Sea and the Bay of Bengal should incorporate such overlooked mechanisms.**

**Keywords:** Arrival times, seismicity, subduction zones, tectonics, tsunami.

THE disaster of 26 December 2004 underscores the need to understand the Indian Ocean tsunami sources. A search for older regional tsunamis exposes the possibility that other potential source zones may exist in the Indian Ocean, as reported by Cummins<sup>1</sup> relating to the earthquake of 1762 off Arakan coast, Burma. Another little-understood potential tsunamigenic source occurs along the Makran subduction zone, which extends 800 km across the northern Arabian Sea (Figure 1). In 1945, a great earthquake ( $M_w$  8.1) struck the coast of eastern Makran near Pasni, followed by a large aftershock in 1947 immediately to the south<sup>2</sup>. A detailed field study of the earthquake had not been attempted at that time, probably hampered by the war. About 4000 people were supposed to have been killed as a cumulative result of the earthquake and the tsunami. The 1945 earthquake of  $M_w$  8.1, with its epicentre located in the offshore of Pasni

(Pakistan), occurred at 21:56 UTC on 27 November, which is about 3 a.m. (local time) on 28 November<sup>3</sup>. Newspaper reports (*The Times of India*, Bombay, 29 November 1945) suggest that the first shock was recorded at the California Institute of Technology, Pasadena at 5:15 p.m. eastern time, which was followed by two shocks 3 and 5 min later.

A convergent margin, the Makran tectonic zone conveys the oceanic part of the Arabian plate beneath the Eurasian plate. This subduction zone that extends along the Gulf of Oman to Baluchistan volcanic arc (Figure 1), has one of the largest accretionary prisms with a wide toe of thick unconsolidated sediments<sup>3</sup>. It forms a shallow-dipping décollement (at a depth of 8.5 km) within a ~4 km thick Himalayan-derived turbidite<sup>4</sup>. General seismicity of the Makran is unusually sparse for a subduction zone, explained as due to the presence of thick sediments and possible high pore pressure and related creep at the shallower levels<sup>3</sup>. However, major historical earthquakes have been reported<sup>5</sup>, and the 1945 earthquake is the most significant

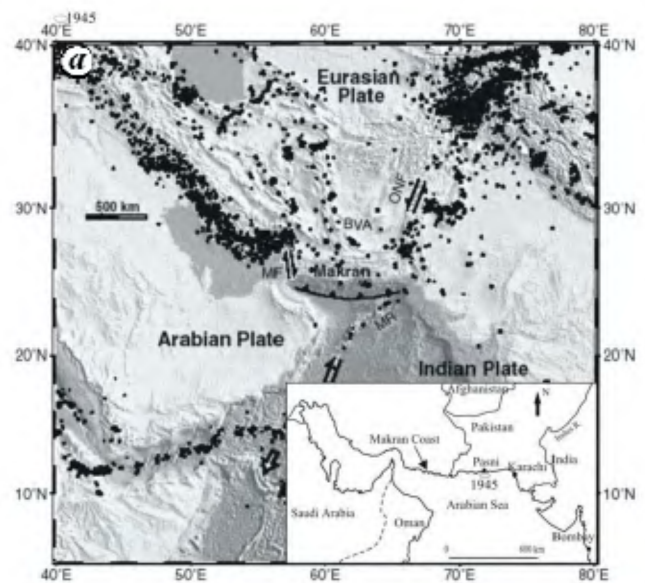


**Figure 1.** *a*, Location map showing tectonic features and earthquakes. *b*, View of the uplifted Makran coast, the flat land in the foreground is elevated about 20 m above the present sea level. The site is about 70 km west of the 1945 earthquake source.

\*For correspondence. (e-mail: cprajendran@ceas.iisc.ernet.in)

recent event with the epicentre located near Pasni (Figure 1). The western part along the Iranian coast appears to be relatively quiet from recent seismicity and no reliable reports are available on large earthquakes from that region.

The 1945 earthquake has source parameters of an interplate thrust event that ruptured about 100 km, approximately one-fifth length of the subduction zone. Byrne *et al.*<sup>3</sup> have mentioned that no uplift data were available from the region other than the reported 2 m uplift at Ormara, after Page *et al.*<sup>6</sup>. According to a dislocation model (a main thrust plane having a seaward up-dip limit with branching coastal imbricate faults) that fits this single observation of coseismic coastal uplift, rupture terminated about 30 km from the offshore, along the shelf edge<sup>3</sup>. The bathymetry indicates that the water depth here is 1000–1200 m. However, Snead<sup>7</sup> has reported that the actual ground uplift at Pasni (near the epicentre) is about 15 ft (4.5 m), contrary to the report of Page *et al.*<sup>6</sup>, which is categorical in asserting that there was no coseismic uplift at Pasni. According to Ambraseys and Melville<sup>5</sup>, the earthquake destroyed 80% of the houses, killing about 45 people. Apart from widespread destruction, their account mentions that the town also witnessed submarine slide which submerged a section of the shore ‘so that the coast today is ~100 m inland’. We do not know if this actually represents the coseismic onshore uplift and corresponding subsidence of the offshore part.

The tsunami generated by this earthquake impacted the coasts of Iran, Oman, Pakistan, and northwest India<sup>8</sup>; it was recorded by tide gauges maintained by the Survey of India at Aden, Karachi and Mumbai<sup>9</sup>. The Indian newspapers also covered the news on the arrival of the tsunami (see Appendices 1 and 2). The tsunami consisted of multiple surges, the second and fourth waves being the largest at Pasni and Karachi respectively<sup>8</sup>. Ambraseys and Melville<sup>5</sup> have mentioned that three waves followed the earthquake. The first one came ashore immediately after the earthquake, but it did not inundate much onto the shore. The last two came 90 and 120 min later around 5:00 a.m. and ‘swept over the one-storey houses at Pasni and Ormara, causing great damage and reaching heights of five to ten meters onshore’. Pendse<sup>8</sup> has assigned greater tsunami heights in Pasni, up to 12–15 m, and has reported that the second wave was the largest, which reached Pasni at 7:15 a.m. Reports, therefore, indicate that there was a substantially long pause between the time of the earthquake and arrival of the tsunami sequence. Recent workers who have examined this event have also commented on this disparity in time<sup>10</sup>. Here, we present the archival data on arrival times of the tsunami and run-up heights at some important ports affected by this event, and compare these arrival times with a wave generation model based on the rupture parameters. We use the source parameters obtained by Byrne *et al.*<sup>3</sup> to suggest a disparity between the origin of the earthquake and the arrival of the tsunami, the latter being delayed by about

30 min at locations within the rupture zone. We argue, based on the mismatch between the computed and actual arrival times of the tsunami, that a submarine landslide induced by the earthquake is a preferred causative mechanism for the tsunami.

The present study uses the finite difference code of TUNAMI-N2 to predict wave propagation<sup>11</sup>. The rupture parameters, as provided by Byrne *et al.*<sup>3</sup>, given in Table 1 were used to model the source of 1945 earthquake and finite difference model. Static displacement on the surface of an elastic half space due to elastic dislocation was computed<sup>12,13</sup>. The governing equations are:

$$\frac{\partial \eta}{\partial t} + \frac{\partial M}{\partial x} + \frac{\partial N}{\partial y} = 0, \quad (1)$$

$$\frac{\partial M}{\partial t} + \frac{\partial}{\partial x} \left( \frac{M^2}{D} \right) + \frac{\partial}{\partial y} \left( \frac{MN}{D} \right) + gD \frac{\partial \eta}{\partial x} + \frac{gn^2}{D^{7/3}} M \sqrt{M^2 + N^2} = 0, \quad (2)$$

$$\frac{\partial N}{\partial t} + \frac{\partial}{\partial x} \left( \frac{MN}{D} \right) + \frac{\partial}{\partial y} \left( \frac{N^2}{D} \right) + gD \frac{\partial \eta}{\partial y} + \frac{gn^2}{D^{7/3}} N \sqrt{M^2 + N^2} = 0, \quad (3)$$

where  $M$  and  $N$  are the discharges in the  $x$  and  $y$  directions respectively,  $h$  the still water depth,  $\eta$  the vertical displacement of water,  $t$  the time,  $g$  the acceleration due to gravity density, and  $D$  the total depth  $D = h + \eta$ .

The computational domain for the study was lat. 4°S–29°N and long. 55°–93°E with a grid spacing of 2 min, which gives 1675 × 1507 grid points (Figure 2). Bathymetry data, GEBCO (General Bathymetry Chart for Ocean), used in the simulation consists of digital average of land and sea-floor elevations from uniform grids assembled into a worldwide dataset with a spacing of 1 minute (both latitude and longitude). Simulations were conducted for 6 h to analyse the propagation along the coast. The maximum water surface elevations for the 6 h simulation indicate the directivity of the tsunami (Figure 3).

**Table 1.** Rupture parameters of the 1945 earthquake<sup>3</sup>

Epicentre longitude (°)	63.48
Epicentre latitude (°)	25.15
Fault length (km)	150
Fault width (km)	70
Slip magnitude (m)	7
Strike angle (°)	246
Rake angle (°)	90
Dip angle (°)	7
Focal depth (km)	15

The synthetic tsunami profiles of water-surface elevations for different coastal stations (Pasni, Muscat, Karachi, Mumbai, Goa, Karwar, Kerala) are shown in Figure 3. The observed wave heights of the 1945 tsunami based on the given source parameters were one magnitude higher than the computed values<sup>14</sup>. Our simulations provide estimates of predicted arrival times at various locations (Table 2, Figure 4). These have been used to understand the discrepancies from those reported (Table 3); only the stations for which we have observed arrival times are discussed in the text.

Historical information indicates that a small surge occurred at Pasni (close to the epicentre) around 4 a.m., followed by a destructive second wave of 12–15 m around 7:15 a.m. We have followed the timings reported by Pendse<sup>8</sup>, because of their agreement with the Survey of India data. The long delay in arrival of the second wave

at the epicentral region (second wave arrived at Pasni and Karachi about 4 h after the earthquake) and the localization of its impact imply that the tsunami surges did not originate coseismically. Another intriguing aspect was that the second wave, which was the largest at Pasni and Karachi, arrived at the latter locality 15 min (7:15 a.m. local time) earlier than at Pasni, the epicentral area.

We interpret the delay in arrival of the tsunami as the time taken for slumping along the continental slope. Theoretical calculations using finite-element models suggest delays of more than 1 h for sediment-layer slumping along moderately dipping continental slopes, causing delayed onset of tsunami<sup>15,16</sup>. The conventional tsunami-generation models are rupture-specific and based on seismic moment and rupture area. These models assume vertical dislocation on the sea floor as the cause of the tsunami. However, potential for tsunami triggering by underwater slides has been recognized for long. The 1958 Lituya Bay, South East Alaska earthquake triggered a subaerial landslide that severely impacted the coast<sup>16</sup>. Other examples include the Papua New Guinea, 1998 and the 1929 Grand Banks, Canada ( $M_w$  7.2) earthquake that caused destructive tsunamis<sup>17</sup>.

As mentioned earlier, the earthquake reportedly caused widespread subaerial sliding and offshore slumping. The extensive breaking of the transoceanic cables<sup>3</sup> implies the slide transforming into turbidity currents as it moved down the slope. Reports of the 1945 tsunami also imply multiple surges with variable wave heights and also complex radiation pattern. Back-scattering (resonance) due to

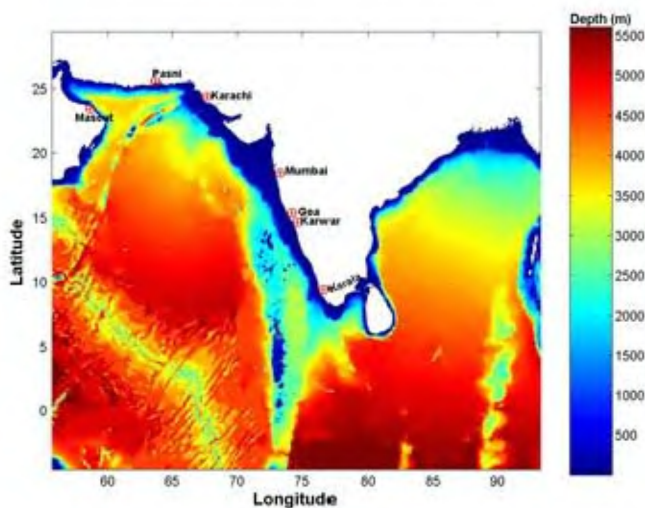


**Figure 2.** Computational domain discretized for numerical simulation. Scale at the right shows depth of water in metres.

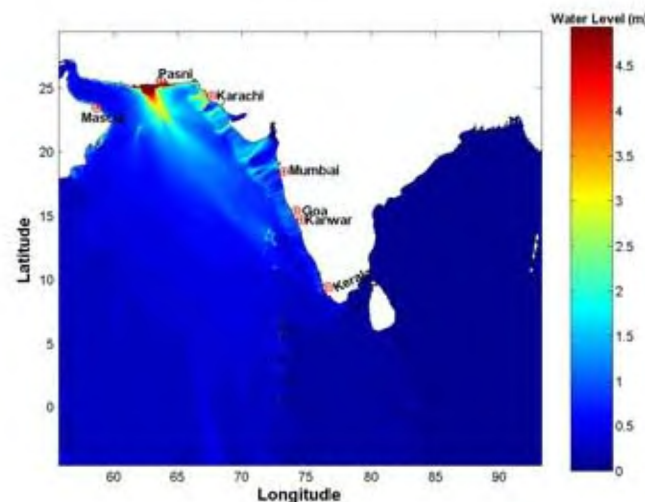


**Figure 3.** Computed model showing maximum offshore tsunami height, following 6 h simulation.

**Table 2.** Simulated arrival times of the 1945 tsunami at various locations

Location	Tsunami arrival time (min)
Muscat (58.46°E, 23.70°N)	45
Pasni (63.27°E, 25.15°N)	5
Karachi (66.80°E, 24.46°N)	106
Mumbai (72.64°E, 18.56°N)	242
Goa (73.54°E, 15.46°N)	204
Karwar (73.88°E, 14.74°N)	215
Kerala (76.70°E, 08.48°N)	259

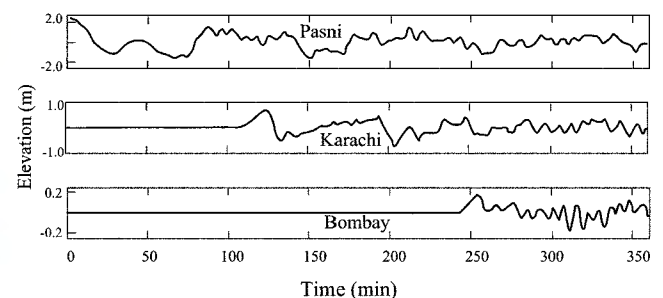


**Figure 4.** Simulated arrival times of the 1945 tsunami at Pasni, Karachi and Bombay (Mumbai).

**Table 3.** Simulated arrival times and delays at various locations

Location	Longitude (°E)	Latitude (°N)	Wave height (m)	Distance (km)	Computed travel time (h:min)	Computed arrival time <sup>a</sup> (h:m:s)	Observed arrival time <sup>b</sup> (h:m)		Delay <sup>c</sup> (h:m)	
							W1	W2	W1	W2 <sup>d</sup>
Pasni/Makran	63.27	25.15	12–15	120	0:05	03:31:55	04:00	07:15	0:28	3:48
Karachi	66.80	24.46	1.35	440	1:46	05:12:55	5:30	07:00	0:17	3:44
Mumbai	72.64	18.56	2.0	1200	4.02	07:28:55	8:15		0:36	

<sup>a</sup>Origin time 3:26:55 plus travel time.<sup>b</sup>W1 and W2: First and second waves.<sup>c</sup>Delay between observed and computed times.<sup>d</sup>Delay between observed arrival time of the first and second wave at Pasni and Karachi.

bathymetric features (between the source and the Arabian Sea coastline) may have also played a role in the directivity of the tsunami and complex radiation, as suggested by Suresh *et al.*<sup>9</sup>.

The reported sequence of events near the source of the 1945 earthquake, however, indicates sediment slumping as the primary cause for the delayed arrivals of the consequent successive tsunamis. The coastal part of the town of Pasni was reported to have slipped south beneath the sea with one of the submarine slides coupled with intense liquefaction; both indicating large-scale ground motion<sup>3</sup>. One remarkable analogy is the 1929 Grand Banks earthquake, where the spatio-temporal growth of the submarine sediment slides along the shelf edge was contributed by strong ground motion<sup>17</sup>.

The submarine slide as an alternate mechanism would not require appreciable displacement on the ocean floor. The mismatch between observed tsunami height and rupture parameters inferred from seismologic data noticed by earlier workers<sup>18</sup> might be explained by this mechanism. The submarine slide scenario may rule out appreciable displacement on the sea floor as the rupture may have terminated at the base of the superjacent turbidite sequence. Alternatively, the maximum coseismic uplift may have occurred closer to the coast, suggesting that the movement along the main thrust (a blind thrust?) terminated nearer to the coast. The Makran event challenges the rupture-centric views on tsunami generation and the hazard preparedness in the Indian Ocean region. Both the Indus and the Bengal fan areas in the north Arabian Sea and the Bay of Bengal respectively, are prone to submarine slides that pose additional tsunami threats in the region, regardless of the rupture dimensions. These points should be factored into the tsunami models for the region.

## Appendix 1

*The Times of India* (29 November 1945, Bombay): ‘Tidal wave hits Bombay shore – entire family washed away – three women drowned in Versova creek’: Fifteen persons were washed away when a huge tidal wave, like of which according to eyewitnesses, has not been experienced in

living memory, hit Bombay’s seashore at 8:15 on Wednesday morning. Of these, two were saved, three were washed up dead and the fate of the remaining ten is unknown.

Four women and one man, all fisherfolk, were overtaken while fishing in knee-deep water at the mouth of the Versova creek, at the northern end of Juhu, and were washed away within the twinkling of the eye . . . Exactly at the same moment, an entire Muslim family consisting of one Rahimtulla, his wife, three children and two servants, was swept away while returning from Haji Ali darga at Mahalaxmi . . . Fakir at the mosque and also fishermen at Juhu say that the phenomenon was strange and unusual . . . there was little time to know what was happening. The upheaval lasted nearly a couple of minutes. The wave then receded.

In Danda and Juhu, a number of small boats were torn off their moorings. The wave in minor form was noted in some parts of Bombay harbour, but no serious damage is reported. A meteorologist suggested that the sudden tidal wave could possibly be due to the buckling of the sea surface by one of the aftershocks of Wednesday morning earthquake, which was of great intensity and had its epicenter about 365 miles from Bombay.

According to Dr H. J. Taylor of Wilson College, the earthquake occurring under the sea would probably affect the level of the seabed and if that were sufficiently widespread, it would certainly result in something of a tidal wave.

Dr Taylor said that, if the earthquake and its reported tidal wave occurred at or about the same time, it seemed probable, indeed, that they were connectible events. It would be difficult to suggest any other explanation for a sudden tidal wave of that kind.

## Appendix 2

*The Times of India* (28 November 1945, Poona): ‘Quake spends fury in sea-tidal wave in Karachi’: Weather experts here believe that the earthquake, which was felt early on Wednesday morning in many parts of India spent its fury in the sea and that only tremors reach the land.

A tidal wave six and half feet in height, swept over the shores of Karachi five hours after the 'quake' shock. It is believed that the 'quake' caused the tidal wave, which took sometime to travel to Karachi.

1. Cummins, P. R., The potential for giant tsunamigenic earthquakes in the northern Bay of Bengal. *Nature*, 2007, **449**, 75–78.
2. Sondhi, V. P., The Makran earthquake 28th Nov. 1945. The birth of new islands. *Indian Miner.*, 1947, **4**, 147–158.
3. Byrne, D. E., Sykes, L. R. and Davis, D. M., Great thrust earthquakes and seismic slip along the plate boundary of the Makran subduction zone. *J. Geophys. Res.*, 1992, **97**, 449–478.
4. Kopp, C., Fruehn, J., Flueh, E. R., Reichert, C., Kukowski, N., Bialas, J. and Klaeschen, D., Structure of the Makran subduction zone from wide-angle and reflection seismic data. *Tectonophysics*, 2000, **329**, 171–191.
5. Ambraseys, N. N. and Melville, C. P., *A History of Persian Earthquakes*, Cambridge University Press, 1982, p. 219.
6. Page, W. D., Alt, J. N., Cluff, L. S. and Plafker, G., Evidence for the recurrence of large-magnitude earthquakes along the Makran coast of Iran and Pakistan. *Tectonophysics*, 1979, **52**, 533–547.
7. Snead, R. E., Recent morphological changes along the coast of West Pakistan. *Ann. Assoc. Am. Geogr.*, 1967, **57**, 550–565.
8. Pendse, C. G., A short note on the Mekran earthquake of the 28 November 1945. *J. Sci. Ind. Res.*, 1948, **5**, 106–108.
9. Suresh, I. *et al.*, The delayed waves of the 1945 Makran tsunami. In Symposium on Giant Earthquake and Tsunamis, Earthquake Res. Inst., Univ. of Tokyo, 2008, S3-1-2.
10. Bilham, R., Lodi, S., Hough, S., Bukhary, S., Murtaza Khan, A. and Rafeeqi, S. F. A., Seismic hazard in Karachi, Pakistan: uncertain past, uncertain future. *Seismol. Res. Lett.*, 2007, **78**, 601–613.
11. Imamura, F., Review of tsunami simulation with a finite-difference method. In *Long-Wave Run-up Models* (eds Yeh, H., Liu, P. and Synolakis, C.), World Scientific, Singapore, 1996, pp. 25–42.
12. Mansinha, L. and Smylie, D. E., The displacement fields of inclined faults. *Bull. Seismol. Soc. Am.*, 1971, **61**, 1433–1440.
13. Okada, Y., Surface deformation due to shear and tensile faults in a half-space. *Bull. Seismol. Soc. Am.*, 1985, **5**, 1135–1154.
14. Geist, E. L., Origin of the 17 July 1998 Papua New Guinea tsunami: earthquake or landslide? *Seismol. Res. Lett.*, 2000, **71**, 344–351.
15. Tsuji, Y., Secondary tsunamis induced by submarine slope slumping triggered by earthquakes in tropical countries. In Symposium on Giant Earthquake and Tsunamis, Earthquake Res. Inst., Univ. of Tokyo, 2008, S3-1-3.
16. Miller, D. J., The Alaska earthquake of 10 July 1958: giant wave in Lituya Bay. *Bull. Seismol. Soc. Am.*, 1960, **50**, 253–266.
17. Hasegawa, H. S. and Kanamori, H., Source mechanism of the magnitude 7.2 Grand Banks earthquake of September 1929: double couple or submarine land slide? *Bull. Seismol. Soc. Am.*, 1987, **77**, 1984–1991.
18. Dominey-Howes, D., Cummins, P. R. and Burbridge, D., Historic records of teletsunami in the Indian Ocean and insights from numerical modeling. *Nat. Hazards*, 2007, **42**, 1–6.

**ACKNOWLEDGEMENTS.** We thank Brian Atwater and the anonymous reviewer for suggestions to improve the manuscript. M.V.R. and N.T.R. thank the Director, ICMAM, Chennai for permission to publish this paper. This work forms an extension of the project funded by INCOIS.

Received 10 June 2008; revised accepted 13 October 2008

## Sensory basis of food perception in tadpoles of the frog, *Sphaerotheca breviceps*

H. S. Sugur, G. S. Mulla, I. R. Purohit, B. A. Shanbhag\* and S. K. Saidapur

Department of Zoology, Karnatak University, Dharwad 580 003, India

**The mechanism of food detection was studied in tadpoles of the frog *Sphaerotheca breviceps* using a rectangular glass tank, the two ends of which served as stimulus zones and housed the food (boiled spinach), providing either visual (food inside a glass beaker) or chemical (food inside a mesh cage wrapped with cheese cloth) cues or both. Each test tadpole (starved for 24 h before the trials) was placed in a centrally kept mesh cage for 5 min to enable perception of food cues. Each trial lasted for 10 min and the time spent by test tadpoles in each stimulus zone was recorded. The tadpoles showed no bias towards any particular side of the apparatus or trial procedure (end bias tests). In tests with visual cues at one end of the test tank also, the tadpoles moved randomly as in end bias tests. In contrast, in tests with chemical cues in one stimulus zone, the tadpoles spent majority of their time near chemical cues of food rather than in the zone that was chemically blank or provided only visual cues. In tests with food in open space in one zone and in the mesh cage in the opposite zone (both providing water-borne chemical cues), the tadpole distribution was random. The findings thus show that *S. breviceps* tadpoles detect food by chemical sensory mechanism rather than visual ones.**

**Keywords:** Food detection, food cues, frog, tadpole.

FORAGING is important in all living organisms for optimum growth, maintenance and reproduction. In most anurans the transitory tadpole stage is designed to exploit the benefits of the aquatic medium in order to gain an optimal size before metamorphosis and taking to terrestrial life. It is basically a food-gathering and growing phase in an aquatic environment. A number of studies have shown that anuran tadpoles respond to chemical, visual or tactile stimuli to elicit appropriate responses<sup>1</sup>. Often the anuran larvae are found in turbid/murky water or water filled with dense vegetation with poor visibility. Further, the tadpoles in general are near-sighted and therefore it is unlikely that they use vision to detect objects at greater distances<sup>1</sup>. Some studies have documented the use of chemical cues in the detection of various stimuli among anuran tadpoles. For instance, tadpoles of *Bufo americanus*<sup>2</sup>, *Rana cascade*, *Rana sylvatica*<sup>3</sup> and *Bufo scaber*<sup>4</sup> are reported to preferentially associate with their siblings

\*For correspondence. (e-mail: bhagyashrishanbhag@gmail.com)